33rd Annual International Conference of the IEEE EMBS
Boston, Massachusetts USA, August 30 - September 3, 2011

Characterization of Subcortical Structures during Deep Brain Stimulation utilizing Support Vector Machines

P. Guillén, F. Martínez-de-Pisón, R. Sánchez, M. Argáez, L. Velázquez

Abstract— **In this paper we discuss an efficient methodology for the characterization of Microelectrode Recordings (MER) obtained during deep brain stimulation surgery for Parkinson's disease using Support Vector Machines and present the results of a preliminary study. The methodology is based in two algorithms: (1) an algorithm extracts multiple computational features from the microelectrode neurophysiology, and (2) integrates them in the support vector machines algorithm for classification. It has been applied to the problem of the recognition of subcortical structures: thalamus nucleus, zona incerta, subthalamic nucleus and substantia nigra. The SVM (support vector machines) algorithm performed quite well achieving 99.4% correct classification. In conclusion, the use of a computer-based system, like the one described in this paper, is intended to avoid human subjectivity in the localization of the subcortical structures and mainly the subthalamic nucleus (STN) for neurostimulation.**

I. Introduction

PARKINSON'S disease (PD) is caused by a depletion of dopamine in the Basal Ganglia region of the brain. PD is most commonly treated by taking L-dopa medication that restores the dopamine levels. Microelectrode guided neurosurgery can also be used for treating PD in severe cases or when medication does not work. These surgical procedures include a pallidotomy or a Deep Brain Stimulation (DBS). During a pallidotomy a lesion is made in the basal ganglia, while in a DBS a lead is implanted to stimulate the neuronal cells in the Basal Ganglia [1].

Surgical approaches to the treatment of Parkinson's disease (PD) have been developed primarily in response to the failure of medical therapies to provide long-term relief from the disabling motor symptoms of the disease. Refined microelectrode recording (MER) techniques allow more detailed physiologic mapping of the subthalamic structures in the operating room, providing more detailed knowledge of electrode location prior to neuroablation or insertion of an implanted deep brain-stimulating lead. The introduction of long-term deep brain stimulation (DBS) as an alternative to irreversible neuroablative procedures may enhance the safety of these procedures while maintaining therapeutic efficacy.

MER signal analysis is largely an art developed and practiced by skilled surgeons who view and listen to the extracellular electrical activity of neurons along a linear trajectory towards the nominal target region. Currently the interpretation of MER signals is primarily performed by the surgeon based on the properties of the MER signals determined by examining the time domain behavior of the signal on oscilloscopes and listening to the signal through conventional speakers. Since the neural activity varies from one structure to another within the brain, the possibility of targeting errors to DBS necessitates the use of some form of intraoperative neurophysiologic monitoring to confirm the correct targeting during surgery [2]-[3].

The purpose of the development of numerical techniques for MER processing is to assist the surgical team in determining the optimal location of the lesion or DBS lead [4]-[6].

Support Vector Machines (SVM) are powerful automatic learning structures, based on the statistical theory of learning, capable of resolving classification, regression and estimation problems. They have been the aim of much research in recent years. The method was proposed by V. Vapnik [7] in the late seventies for solving pattern recognition problems. In the 1990s, use of the method became widespread [8] and it is currently the object of great interest. Support Vector Machines offer improvements over traditional learning methods: the size of the network is not established from the outset and the maximum generalization level is guaranteed mathematically.

This work presents supervised machine learning to integrate multiples features. Specifically, we use 6 mathematical features [6], each measuring different characteristics of the signals from the microelectrode recordings, in order to quantify changes in neural activity from subcortical structures, and that could be used in DBS.

II. Materials and Methods

A. Data Base

Intra-operative acquisitions were made on unmedicated awake patients that underwent DBS implantation. Four patients aging 55±6 (4 male and 1 female) who signed informed consent participated. Microelectrode recordings were made using the ISIS MER (System Innomed Medical GmbH). Visualization of neural data started 10 mm above

Manuscript received April 15, 2011. This work was supported in part by the U.S. Army Research Laboratory, through the Army High Performance Computing Research Center, Cooperative Agreement W911NF-07-0027 and Universidad de Los Andes, Merida, Venezuela.

P. Guillén, Program in Computational Sciences, University of Texas at El Paso, TX, 79968, USA, pguillen@utep.edu, Universidad de Los Andes, Merida, Venezuela.

F. Martínez-de-Pisón, EDMANS Research Group, University of La Rioja at Logroño, La Rioja, 26004, Spain, http://www.mineriadatos.com

R. Sánchez, Program in Computational Sciences, University of Texas at El Paso, TX, 79968, USA, reinaldosanar@gmail.com

M. Argáez, Program in Computational Sciences, University of Texas at El Paso, TX, 79968, USA, margaez@utep.edu

L. Velázquez, Program in Computational Sciences, University of Texas at El Paso, TX, 79968, USA, leti@utep.edu

the target data. Every 1 mm one new site was created if the distance between the microelectrode and the target point was larger than 3 mm. At distances less than 3 mm, sites were created every 0.5 mm. MER signals were labeled by specialists in neurosurgery and neurophysiology. At each site the acquisition lasted 2s with sampling frequency of 25 kHz and 16-bit of resolution. In total, there are 52 neural recordings divided in four classes: 13 signals from thalamus nucleus, 13 signals from subthalamic nucleus, 13 signals from substantia nigra, and 13 from zona incerta. These procedures were performed by the Institute of Parkinson and Epilepsy of the Eje Cafetero of Pereira, Colombia. Figures 1, 2, 3, and 4 show MER for thalamus, zona incerta, subthalamic nucleus and substantia nigra, respectively.

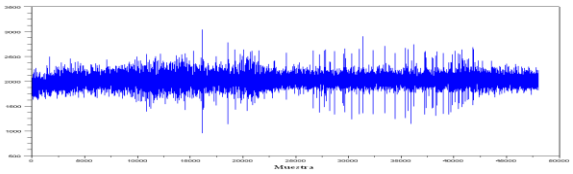

Fig. 1. MER-Thalamus.

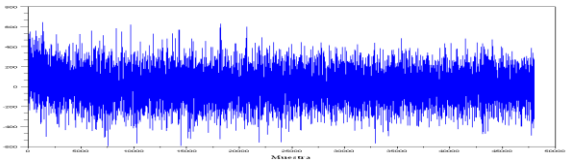

Fig. 2. MER-Zona Incerta.

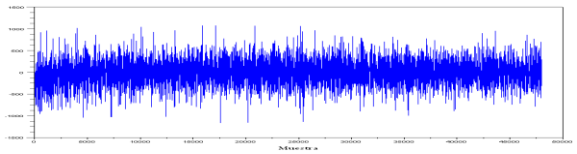

Fig. 3. MER-Subthalamic Nucleus.

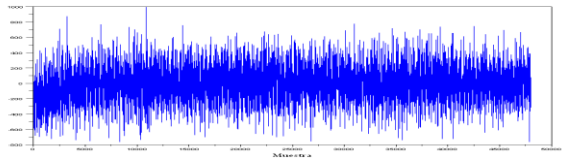

Fig. 4. MER-Substantia Nigra.

B. Computational Features

The following is a brief description of each feature and the corresponding formula for its calculation [6]. In the following, X is the data epoch vector of length N.

Curve Length

This feature is used to capture the stability of the values of a signal. If the value of this feature is low in an interval, provided by the user, the signal is stable, if not, the signal is unstable. Equation (1) defines the calculation of this measure:

$$L = \sum_{i=1}^{N-1} \left| x_{i+1} - x_i \right| \tag{1}$$

where each x_i is a sample of the dataset $X = (x_1, x_2, ..., x_N)$.

Threshold

The determination of the threshold γ is based on the calculation of the deviation of the data to capture how the data in a window of size N are scattered. The threshold is determined by:

$$\gamma = \frac{3}{N-1} \sqrt{\sum_{i=1}^{N} \left(x_i - \bar{X} \right)^2} \tag{2}$$

where $\bar{X}$ it is the average of the dataset.

Peaks

The number of peaks whose value is positive is determined by:

$$\kappa = \frac{1}{2} \sum_{i=1}^{N-2} max \left\{ 0, \left| sgn\left[x_{i+1} - x_i \right] - sgn\left[x_{i+2} - x_{i+1} \right] \right| \right\} \tag{3}$$

where

$$max(a,b) = \begin{cases} a & if \quad a > b \\ b & if \quad a < b \\ a \ o \ b & if \quad a = b \end{cases}$$

$$sgn(x) = \begin{cases} 1, & if \quad x > 0 \\ 0, & if \quad x = 0 \\ -1, & if \quad x < 0 \end{cases}$$

Root mean square

Defined as the square root of the average of the sum of the squares of the signal. The root mean square value is determined by:

$$\delta = \sqrt{\frac{\sum_{i=1}^{N} x_i^2}{N}} \tag{4}$$

Average of nonlinear energy

The average of the non-linear energy is determined by:

$$\Psi = \frac{1}{N-2} \sum_{i=2}^{N-1} x_i^2 - x_{i-1} x_{i+1} \tag{5}$$

Zero crossings

The numbers of zero crossings k for one signal is determined by:

$$\kappa = \frac{1}{2} \sum_{i=1}^{N-1} \left| sgn\left(x_{i+1} \right) - sgn\left(x_i \right) \right| \tag{6}$$

C. Support Vector Machines

The Support Vector Machines (SVM) approach is a novel algorithm for data classification and regression. It was introduced by Vapnik in 1995 [7] and is clearly connected with statistical learning theory [8]. The SVM is an estimation algorithm that separates data in two classes, but since all classification problems can be restricted to consideration of the two-class classification problem without loss of generality, SVM can be applied in classification

problems in general. Basically, SVM only use information (examples) within the decision borders (called *support vectors*) and, by means of quadratic programming (QP), they attempt to induce linear or hyperplane separators which maximize the minimum distance between classes. In order to process non-linear ratios, SVM uses kernel functions to project the information in spaces of greater dimensionality and then transform them into linearly separable classes (Fig. 5). The SVM algorithm is a learning machine, therefore it is based on training, testing and performance evaluation, which are common steps in every learning procedure. Training involves optimization of a convex cost function where there are no local minima to complicate the learning process. Testing is based on the model evaluation using the support vectors to classify a test dataset. Performance is based on error rate determination as test set data size tends to infinity.

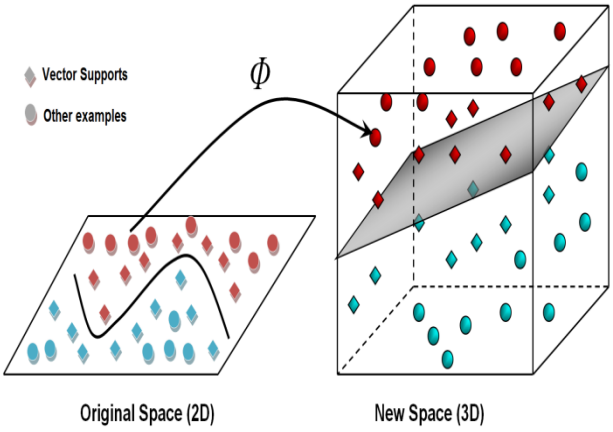

Fig. 5. Example of instances projection from original space (2D) to a greater dimension space (3D) in order to linearly separate the classes.

D. Computational Implementation

As mentioned when describing the database, each recording was acquired for 2 seconds at 24 KHz sampling frequency, which leads to each recording having 48,000 samples. Considering a trajectory of 13 records for each of the subcortical structures, the final trajectory is made up of 52 recording and has a total of 2,496,000 samples. Then the final trajectory is divided into consecutive windows of 4,992 samples and for each of these windows we determined the six computational features (statistical indexes), obtaining a total of 500 instances (patterns) per feature. This is presented in matrix form follows:

$$X = \begin{array}{c} \\ X_1 \\ X_2 \\ \vdots \\ \vdots \\ X_n \end{array} \begin{array}{c} \begin{array}{cccccc} V_1 & V_2 & \cdots & \cdots & V_p \end{array} \\ \begin{bmatrix} x_{11} & x_{12} & \cdots & \cdots & x_{1p} \\ x_{21} & x_{22} & \cdots & \cdots & x_{2p} \\ \vdots & \vdots & \ddots & \cdots & \vdots \\ \vdots & \vdots & \cdots & \ddots & \vdots \\ x_{n1} & x_{n2} & \cdots & \cdots & x_{np} \end{bmatrix} \end{array}$$

Fig. 6. Data matrix *X*.

where $n = 500$ instances y $p = 6$ variables or computational features.

The data matrix is assembled so that the first 125 instances correspond to the thalamus nucleus, the second 125 instances correspond to the zona incerta, the third 125 correspond to the subthalamic nucleus and finally the last 125 instances correspond to the substantia nigra.

Statistical indexes or computational features of this work were scheduled in the Scilab 5.3.0 programming language and used with the package Weka 3.7 algorithm SMO [9] to perform the classification using SVM.

III. RESULTS

Gaussian and polynomial kernels, with different parameter values, were used in order to obtain the best SVM model. The best model was the one which reached the highest value of Kappa statistic *K* using *n*-fold cross validation.

n-fold cross validation methodology allows us to obtain realistic errors using the complete database. Cross-validation consists of dividing the initial database into *n* subsets and selecting *n*-1 subsets to create the model. The subset not used in the process is used to calculate a partial sample error. This procedure is repeated *n* times, each time using a different test subset. Finally, the error is calculated by the arithmetic mean of the *n* partial samples errors. In this work, *n*=10.

The Kappa statistic *K* is one of the most widely-used parameters. This coefficient determines the degree of agreement between categorical variables. It is a more robust parameter than the percentage of correctly classified examples (*Precision*) since *K* also takes into account those cases in which agreement occurs by chance. Thus, a *K* value of 1.0 represents a statistically perfect model while *K*=0 is the value expected for a model obtained by chance. According to some authors [10], *K* can be considered excellent for values greater than 0.75, good between 0.40 and 0.75 and poor for values below 0.40.

Other parameters were used to evaluate the models prediction capacity. *Precision* is one of these parameters, defined as the proportion of examples correctly classified divided by all the elements that were classified for this class. *Recall* is defined as the proportion of examples correctly classified divided by all elements of this class. *F-Measure* is the harmonic mean of *Precision* and *Recall*. Values of these parameters close to one indicate good accuracy in the predictions for each class.

In order to obtain the best model, different values of the complexity parameter *C* were tested with $C = 10^k$ where *k* values were from –3 to 3 with a step of 0.2 (31 values). Also, different values of the exponent (*e*) for the *polynomial kernel* and gamma (*g*) for the *Gaussian kernel* were used. In particular, *e* values were 1, 2 and 3, and *g* values were 0.005, 0.01, 0.02, 0.03, 0.05 and 0.1. Therefore, the number of models trained with *polynomial kernel* was ninety three ($C \times e = 31 \times 3 = 93$) and with *Gaussian kernel* was one

hundred eighty six ($C \times g = 31 \times 6 = 186$).

The results of the best model obtained with *polynomial kernel*, C = 10.0 and e = 1 are shown in Figure 6. In this figure is possible to observe that the SVM model was able to classify correctly 497 (99.4%) from a total of 500 instances. Parameters like *Precision* or *Recall*, with values over 0.99 for the four classes (*thalamus nucleus*, *zona incerta*, *subthalamic nucleus* and *substantia nigra*), would be considered excellent. Also, the ROC-Areas values were very high. Finally, in the Confusion Matrix we can observe that only three cases were not classified correctly and according to *K,* the best model obtained was excellent (K = 0.992).

IV. Conclusion

This work presented the results of a preliminary study making use of two methodologies for the characterization of subcorticals structures from Parkinson's patients.

The results obtained show how the computational features applied in this work a MER from Parkinson's patients are able to extract, quantify and differentiate the information contained of the neural activity between the subcortical structures.

After obtaining the computational features for each subcortical structures, and using them on the SVM algorithm for classification, the results showed that SVM was be able to classify correctly 497 (99.4%) from the 500 instances.

Finally, various parameters to evaluate the prediction capacity of the model were obtained, indicating good accuracy in the predictions for each subcortical structure (class).

Since the neural activity varies from one structure to another within the brain, the possibility of targeting errors to DBS necessitates the use of some form of intraoperative neurophysiologic monitoring to confirm the correct targeting during surgery, so that the use of methodologies from data mining like the one presented in this work could be used in the process of localization of the subcortical structures and mainly the subthalamic nucleus (STN) for neurostimulation.

Acknowledgment

This work was supported in part by the U.S. Army Research Laboratory, through the Army High Performance Computing Research Center, Cooperative Agreement W911NF-07-0027, Universidad de Los Andes, and the Program in Computational Science at the University of Texas at El Paso. The author thanks the Institute of Parkinson and Epilepsy of the Eje Cafetero of Pereira in Colombia for supplying the data recordings.


```
Time taken to build model: 0.75 seconds

=== Stratified cross-validation ===
=== Summary ===

Correctly Classified Instances         497               99.4    %
Incorrectly Classified Instances         3                0.6    %
Kappa statistic                          0.992
Mean absolute error                      0.2507
Root mean squared error                  0.3126
Relative absolute error                 66.8405 %
Root relative squared error             72.1989 %
Coverage of cases (0.95 level)         100      %
Mean rel. region size (0.95 level)      75.25   %
Total Number of Instances              500

=== Detailed Accuracy By Class ===

               TP Rate   FP Rate   Precision   Recall  F-Measure   ROC Area  Class
                 1         0          1        1         1          1        Thalamus
                 0.992     0.003      0.992    0.992     0.992      0.996    Zona Incerta
                 0.992     0.003      0.992    0.992     0.992      0.997    Subthalamic Nucleus
                 0.992     0.003      0.992    0.992     0.992      0.995    Substantia Nigra
Weighted Avg.    0.994     0.002      0.994    0.994     0.994      0.997

=== Confusion Matrix ===

   a   b   c   d   <-- classified as
 125   0   0   0 |   a = Thalamus
   0 124   0   1 |   b = Zona Incerta
   0   1 124   0 |   c = Subthalamic Nucleus
   0   0   1 124 |   d = Substantia Nigra
```

Fig. 6. 10-folds cross-validation results obtained with the best SVM model.

References

[1] C. Shin-Yuan, L. Sheng-Huang, L. Shinn-Zong, Subthalamic Nucleus Deep Brain Stimulation for Parkinson's Disease – An Update Review. Tzu Chi Med J, 2005, 17, (4), pp. 205-212.

[2] C. Pollo, F. Vingerhoets, E. Pralong, J. Ghika, P. Maeder, R. Meuli, J. Thiran, J. Villemure, Localization of electrodes in the subthalamic nucleus on magnetic resonance imaging. J Neurosurg, 2007,106, pp. 36-44.

[3] J. Sanchez Castro, C. Pollo, O. Cuisenaire, J. Villemure, J. Thiran, Validation of experts versus atlas-based and automatic registration methods for subthalamic nucleus targeting on MRI. Int J CARS, 2006, 1, pp. 5-12.

[4] A. Pesenti, M. Rohr, M. Egidi, P. Rampini, F. Tamma, M. Locatelli, E. Caputo, V. Chiesa, A. Bianchi, S. Barbieri, G. Baselli, A. Priori, The subthalamic nucleus in Parkinson´s disease: power spectral density analysis of neural intraoperative signals. Neurol Sci, 2003, 24, pp. 367-374.

[5] J. Luján, A. Noecker, C. Butson, S. Cooper, B. Walter, J. Vitek, C. McIntyre, Automated 3-Dimensional Brain Atlas Fitting to Microlectrode Recordings from Deep Brain Stimulation Surgeries. Stereotact Func Neurosurg, 2009, 87, pp. 229-240.

[6] S. Wong, G. Baltuch, J. Jaggi, S. Danish, Functional localization and visualization of the subthalamic nucleus from microelectrode recordings acquired during DBS surgery with unsupervised machine learning. J. Neural Eng, 2009, 6, pp. 1-11.

[7] V. Vapnik, The nature of statistical learning theory, 2nd ed. Springer-Verlag, New York, 2000.

[8] B. Boser, I. Guyon, V. Vapnik, A Training Algorithm for Optimal Margin Classifiers, in Proceedings of the NAFIPS'99, 1999, pp. 580-584.

[9] M. Hall, E. Frank, G. Holmes, B. Pfahringer, P. Reutemann, H. Witten, The WEKA Data Mining Software: An Update. SIGKDD Explorations, 2009, 11, pp. 10-18.

[10] J. Fleiss, Statistical methods for rates and proportions, 2nd ed. John Wiley, New York, 1981.